

Magnetic Modeling of a Mutually-Coupled Two-Finger Variable Reluctance Gripper

Norbert C. Cheung, *Member IEEE*
eencheun@poly.edu.hk

Kenneth Kin-Chung Chan, *Student IEEE*
98901131r@poly.edu.hk

Department of Electrical Engineering
The Hong Kong Polytechnic University
Hung Hom, Kowloon, HONG KONG

Abstract—Variable reluctance actuators have been used widely as low-cost, on-off type mechanical actuators, due to their inherent advantages of rugged-construction and ease-of-manufacture. This paper reports on the investigation work of applying variable-reluctance principle to the design of a novel two-finger gripper. Contrary to previous on-off type variable reluctance devices, the proposed actuator can be operated in position-control, velocity-control, and force-control modes. To enable effective control of the two-finger variable-reluctance gripper, its electromagnetic and mechanical properties have to be fully investigated, and an efficient model has to be constructed.

Since the forces on the two fingers of the gripper are produced by the variation of flux, and flux is a nonlinear quantity, the electro-magnetic characteristics of the two-finger gripper are much more complex than other types of devices (e.g. permanent magnet voice coil). Moreover, the existences of coupling effects make the characterization of the gripper even more complicated. In the past, most mutual coupling effects in variable reluctance machines are neglected for the sake of simplicity. However, due to the unique structure of the two-finger variable-reluctance gripper, it was found that mutual coupling can constitute significant modeling discrepancy.

The work described in this paper is the first of its kind to carry out a detail study on the electromagnetic properties of a tightly-coupled two-finger variable-reluctance gripper, including its mutual-coupling effects. In the study, the flux modeling of a mutually coupled variable reluctance gripper is carried out. Magnetic equations of the actuator structure are derived and the flux model is constructed. To verify the study results, a similar two-finger variable-reluctance gripper was fabricated and its electro-magnetic characteristics were measured. When the measured results were compared with the model simulation, it was found that the two sets of data matched quite well with each other and confirmed that the model was an accurate representation of the two-finger variable-reluctance gripper.

The investigation work describes in this paper enables a better understanding of mutually-coupled limited-stroke variable-reluctance actuators. Furthermore, it produces an effective simulation model for the future design and control of this class of device.

I. INTRODUCTION

Variable reluctance motor (VRM) has drawn much research attention over the past decade, due to its robust and low-cost structure, and the potential for numerous industrial applications. However, VRM has an inherent nonlinear characteristics; problems of torque-ripple and non-uniform force will occur when it is driven by standard motor drives. During the past few years, many publications on the improvements of VRM designs, commutation methods and specialized drives have emerged. These methods were made possible by the advancement of simulation tools and computer

processing power. Now, it is possible to include most of the nonlinear side-effects into the construction and simulation of the VRM model, and the real-time control of the VRM hardware.

One of the side-effect is mutual coupling. For the sake of simplicity, this side-effect has always been neglected in the model simulation and the real-time control. As a result, the VRM will not achieve satisfactory performance under precision control applications. Recently, numerous FEM analysis and simulation results have shown that mutual flux linkage plays an important role in the VRM modeling [1-5]. [6] and [7] have shown that the Switched Reluctance Motor models would be more accurate and useful if mutual flux linkage was taken into account. Moreover, the existence of mutual inductance can influence the current dynamics of the motor. Without an accurate representation, current controller will not be optimized and torque ripple will appear.

This paper describes the modeling of a mutually-coupled two-finger VR gripper. The novel gripper is designed to pick and place delicate objects in robotics applications. Unlike the commonly used on-off type variable reluctance actuators in the market, the proposed actuator are designed to operate in position-control, velocity-control, and force-control modes under high precision. Due to these requirements, a detail study on the electromagnetic characteristics of the gripper is necessary, and an accurate model is needed. The tightly-coupled finger structure has made the mutual coupling side-effect constituted significantly to the modeling discrepancy. Therefore an investigation on the mutual coupling of the two coils of the actuator is required and its effect should be included into the model.

In this paper, the proposed structure of the two-finger VR gripper is described in section II. The reluctance modeling of the device is described in section III. Air-gap permeances analysis and magnetic circuit analysis of the VR gripper are described in sections IV and V respectively. The actual construction of the VR gripper and its flux simulation result are presented in section VI. The experimental procedure to acquire the magnetic characteristics of the actuator is described in section VII. Finally, the measured results are shown in section VIII. The results confirmed that the flux model of VR gripper developed is effective, efficient, and accurate.

II. PROPOSED VR GRIPPER STRUCTURE

Fig. 1 shows the structure of the two-finger VR gripper. It

consists of two rotary elements, each attached to a finger. The stator contains two coils, each with a 400-turn winding.

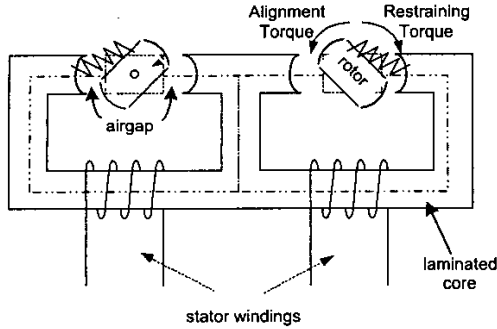


Fig. 1. Proposed VR Finger Gripper

The moving rotors are mounted onto two individual shafts, whose axes are normal to the plane of the diagram, so that the moving elements may rotate freely between the poles of the stator. Both the rotors and stators are made up of laminated mild steel to reduce eddy currents.

The two fingers of the gripper, shown in Fig. 1, are 90mm long and are spring loaded. This arrangement allows bi-directional movement from a single-direction coil excitation. When currents are applied to the stator windings, the rotors will rotate away from initial rest positions to reduce their reluctance by alignment torque. The rotors will stop when alignment torque comes into equilibrium with restraining torque provided by the spring. When the fingers rotate by 70°, the fingertips would be closed. Incremental rotary encoders are mounted on the actuator's shafts to measure the rotor positions with a resolution of 0.09°.

The overall construction is extremely simple and robust, and it is very similar to the rotary solenoids used simple on-off mechanical actuation devices. Combining the two fingers into a single magnetic housing has made the finger alignment process much simpler and the overall size much smaller.

III. RELUCTANCE MODEL

The forces of the two fingers are produced by the variation of reluctance on the magnetic circuit. The idealized reluctance variation of each of the finger can be expressed as a sinusoidal variation, as shown in Fig. 2.

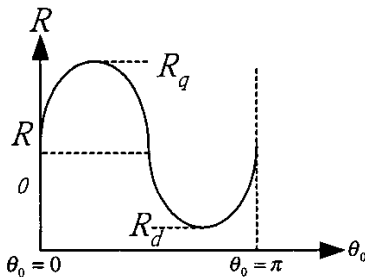


Fig. 2. Reluctance Variation of VR gripper

The graph can be expressed in equation form [8] as (1):

$$R = \frac{1}{2}(R_q + R_d) - \frac{1}{2}(R_q - R_d) \cos 2\theta_0 \quad (1)$$

θ_0 is the instantaneous rotor position, R_d and R_q refers to the minimum and maximum value of reluctances, namely, direct-axis reluctance and quadrature-axis reluctance. R_d is directly in line with the axis of the stator poles.

IV. AIR-GAP PERMEANCES

Air-gap permeances determine most of the flux within the magnetic circuit. Air-gap model consists of overlap and leakage permeances [1]. Permeance can be expressed as:

$$G = \frac{1}{\mathcal{R}} = \frac{\mu_0 A}{g} \quad (2)$$

where G , R , μ_0 , A and g are permeance, reluctance, permeability of air, cross-sectional area of magnetic path and air-gap distance.

A) Overlap Permeance

Fig. 3 shows mechanical diagram of the VR gripper, which contains notations. Overlap permeance can be described by its cross-sectional area and maximum permeance, as shown in (3) and (4).

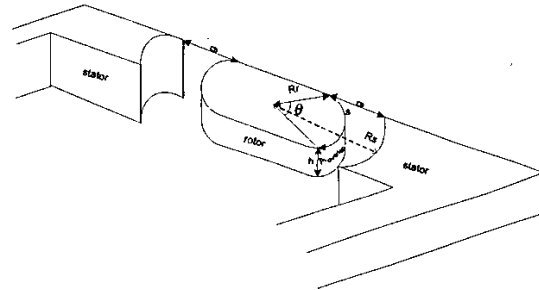


Fig. 3. Mechanical Diagram of VR Gripper

The cross sectional area of the airgap, $A_{overlap}$ can be written as:

$$\begin{aligned} A_{overlap} &= sh \\ &= R_r \theta \cdot h \\ &= \frac{(R_r + R_s)}{2} \cdot \theta h \end{aligned} \quad (3)$$

where θ is maximum permissible overlap angle, h is axial

length of rotor. Radii R_r and R_s belong to the rotor and stator pole faces respectively.

When rotor is fully aligned with stator core, maximum permeance, G_{max} can be obtained as:

$$G_{max} = \frac{\mu_0 A}{airgap} = \frac{\mu_0 \theta h}{2g} \cdot \frac{(R_r + R_s)}{2} \quad (4)$$

When rotor is partially overlap with stator core by $\theta_{overlap}$ angle, overlap permeance, $G_{overlap}$ can be represented as:

$$G_{overlap} = G_{max} \frac{\theta_{overlap}}{\theta} \quad (5)$$

B) Fringing Permeance

Fringing permeance can be occurred when either there is overlap or no overlap between rotor and stator. Fig. 4 shows the fringing flux path when rotor overlaps stator.

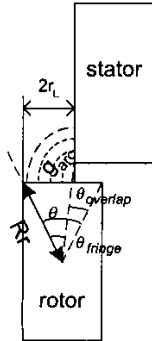


Fig. 4. Leakage path of VR gripper

Case 1: With overlap

In this case, the flux tube can be approximated by a 90° wedge [1].

$$r_L = R_r \frac{\theta_{fringe1}}{2} \quad (6)$$

where $\theta_{fringe1}$ is the non-overlap angle. The cross sectional area of the wedge $A_{fringe1}$ can be represented as:

$$A_{fringe1} = 2R_r \theta_{fringe1} h \quad (7)$$

Combining Equations (5) and (6), fringing permeance with overlap can be simplified as:

$$G_{fringe1} = \frac{\mu_0 A_{fringe1}}{g} = \frac{4\mu_0 h}{\pi} \quad (8)$$

Case 2: Without overlap

Fig. 5 shows the fringing flux path when no overlap is found between rotor and stator. Flux path here can be considered as a combination of fringing and overlap permeances, which can be separated as area 1 and 2 respectively. Cross sectional area, $A_{fringe2}$ in this context is same as the surface area of the pole face. This can be represented as equation below:

$$A_{fringe2} = R_r \theta h \quad (9)$$

Air-gap for area 1 and 2 can be represented as:

$$g_{fringe2} = \frac{\pi R_r \theta + \theta_{space} (R_r + R_s)}{2} \quad (10)$$

As result, fringing permeance without overlap, $G_{fringe2}$ can be obtained by combining (8) and (9).

$$G_{fringe2} = \mu_0 \frac{A_{fringe2}}{g_{fringe2}} \quad (11)$$

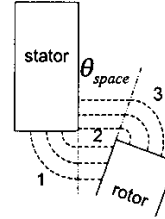


Fig. 5. Fringing flux path without overlap

C) Stator Core Leakage Permeance

Leakage flux path is depicted in Fig. 6. And stator core leakage permeance can be expressed as:

$$G_{leakage} = \frac{\mu_0 r h}{g_{leakage}} \quad (12)$$

where r , h and $g_{leakage}$ are length of stator core limb, thickness of stator core and distance of leakage air-gap respectively.

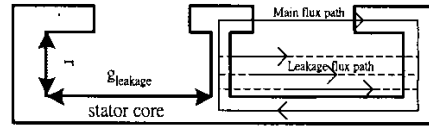


Fig. 6. Leakage flux path of VR gripper

V. MAGNETIC CIRCUIT ANALYSIS

Fig. 7 shows the magnetic representation of the proposed VR gripper. The stator coils, rotor and E-core common path can be represented by two MMF sources F_l and F_r , a fixed reluctance R_f and two variable reluctances R_v .

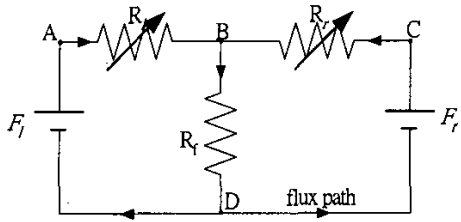


Fig. 7. Magnetic Representation of the proposed VR Gripper

Fig. 8 shows one of the operation case, when the stator windings are excited in different directions. Due to the symmetrical structure of the actuator, the excitation currents in gripping motion in both stator windings and thus the MMF sources, F_l and F_r are assumed to be equal. Besides, both rotors have same cross-sectional area and air-gap; both variable reluctance, R_l and R_r can also be assumed equal. In other words, the magnetic circuit can be simplified as Fig. 8 with R_l and R_r , which represents fixed and variable reluctances.

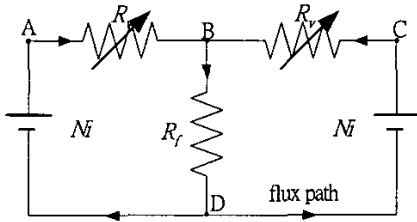


Fig. 8. Simplified Magnetic Representation of the proposed VR Gripper

As shown in Fig. 8, fixed reluctance R_f refers to the reluctance of common flux path BD, while the variable reluctance R_v refers to reluctance due to air-gap and fringing permeances.

By superposition, F_l and F_r can be considered separately. Individual effect can be summed up afterwards. Fig. 9 and 10 shows superposition of VR gripper magnetic circuit with left and right MMF sources respectively.

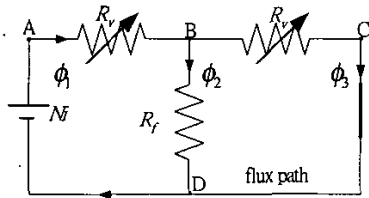


Fig. 9. Superposition of VR gripper magnetic circuit with left MMF source only

In Fig. 9, only left MMF source F_l is considered and F_r is removed and short-circuited. ϕ_1 flows through reluctance R_v between node AB and proportionally divided into ϕ_2 and ϕ_3 . Similarly, in Fig. 10, ϕ_3 flows through reluctance R_v between node AB and proportionally divided into ϕ_2 and ϕ_1 .

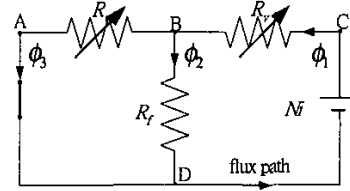


Fig. 10. Superposition of VR gripper magnetic circuit with right MMF source only

The magnetic circuit can then be expressed as:

$$F_l = NI = (\phi_1 - \phi_3)R_v + \phi_2 R_f \quad (13)$$

where F, N, I, Φ, R_f, R_v correspond to MMF source, no of turns in stator winding, stator current, flux, variable and fixed reluctances respectively.

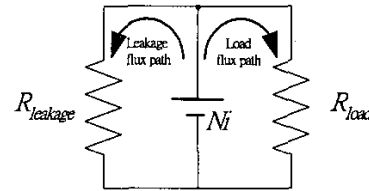


Fig. 11. Leakage flux magnetic representation of the proposed VR Gripper

Fig. 11 shows the leakage flux magnetic representation of the proposed VR gripper. The leakage reluctance, $R_{leakage}$, can be viewed as an internal resistance of a voltage source, which parallel with the equivalent load. In this context, the leakage reluctance parallels with the MMF source and leakage flux flows through it. As a result, net flux flow through the equivalent reluctance load of the circuit is reduced. Consequently, (13) can be revised as follows:

$$F_l = NI = (\phi'_1 - \phi_3)R_v + \phi_2 R_f \quad (14)$$

where ϕ'_1 represents the net flux flows through the equivalent reluctance load of the magnetic circuit.

VI. FLUX SIMULATION

Fig. 12 shows the construction of the VR gripper at (a) grasp and (b) release positions respectively.



(a) at grasp position (b) at release position
Fig. 12. The VR Finger Gripper

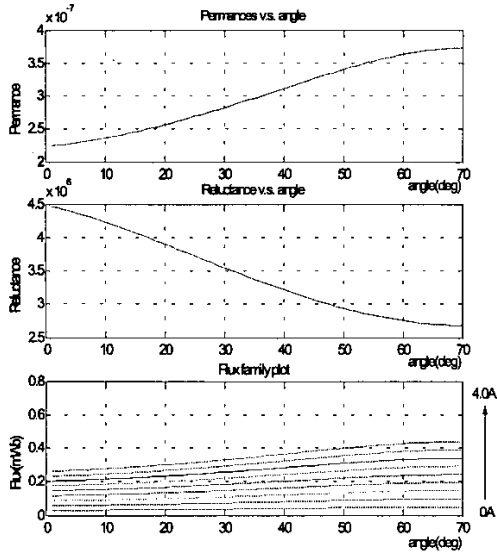


Fig. 13. Flux Simulation of the VR gripper at different current and angles VR gripper profile is tabulated below:

	Notation	Values
Rotor air-gap	g	1mm
Rotor edge to rotor centre	R_r	17mm
Stator edge to rotor centre	R_s	18mm
Core height	h	15mm
Angular Travel	θ_{travel}	70°
Rotor Core angle	θ	60°
Max. Overlap angle	$\theta_{overlap}$	45°
Non-overlap angle	θ_{space}	25°
Stator Windings	N	400 turns
Max. Continuous Current	I	4A

Table 1. VR Gripper Profile

By combining all the mentioned magnetic equations in previous sections, a flux model of a VR gripper can be constructed. Fig. 13 shows the simulated variable permeance, variable reluctance and flux flow through it at different current level versus different angular positions.

At initial position, the rotor is at unaligned position. As angle increases, permeance increases and reluctance is reduced. The pattern of variation is described in (1). Flux also increases as angles and current increase. However, flux increases at a faster rate as angle becomes larger, i.e. reluctance is smaller.

VII. MAGNETIC CHARACTERISATION EXPERIMENT

When a flux passes through a coil with N_s turns, an electromotive force (EMF), $e(t)$, would be induced. Flux $\Phi(t)$ can be expressed as:

$$\Phi(t) = -\frac{1}{N_s} \int e(t) \cdot dt \quad (15)$$

Motor windings are excited with an AC current with the rotor

kept still. Frequency is chosen at 50Hz and different current levels can be adjusted with an isolated autotransformer. Current is measured with a current resistor. Search coils, S1, S2 and S3 are wound around the stator to determine the flux level.

A dSPACE DS1102 card is used as data acquisition controller. The card has an on-board 60MHz TMS320C31 DSP for real-time computation and interfaces with the PC through the ISA bus. It consists of two 24bits incremental encoder input channels, four ADC and six PWM channels. In connecting with MATLAB real-time workshop and SIMULINK, real-time control C-code can be generated with a SIMULINK diagram. Assembly codes can be compiled and downloaded to the DSP.

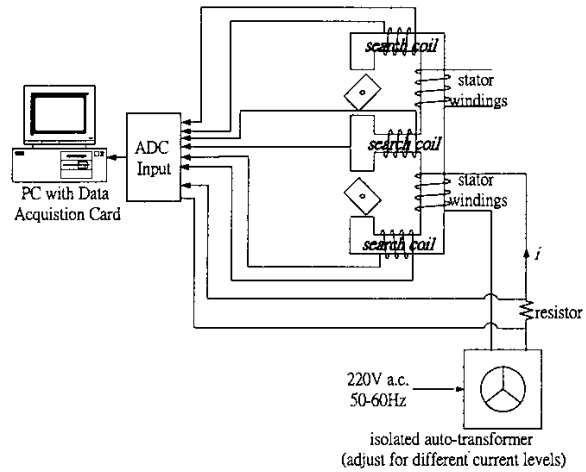


Fig. 14. Experimental Setup for magnetic characterisation

Search coil induced voltage and current levels are filtered, amplified and fed into the ADC channels. Encoders are also connected to the encoder channel to high precision reading.

Since flux linkage is a function of self and mutual rotor positions and its corresponding stator winding current, i.e. $\lambda = f(\theta, \theta_m, i_s)$. With this 3D problem, it is not possible to measure and build up a 3D lookup table, which is extremely costly and impossible to measure. Simplification of the problem complexity is necessary.

Similarly, it is assumed that under gripping motion, both rotor angles are equal and reduced the problem complexity to a 2D level. Flux is measured with stator current ranging from 0.5A to 4A and angular positions from 0° to 70°.

VIII. RESULTS

Fig. 15 and 16 shows the hysteresis loops of VR gripper at different current levels and angular positions respectively. By choosing all the vertex of the hysteresis loops, actual flux of the VR gripper can be plotted as Fig. 17.

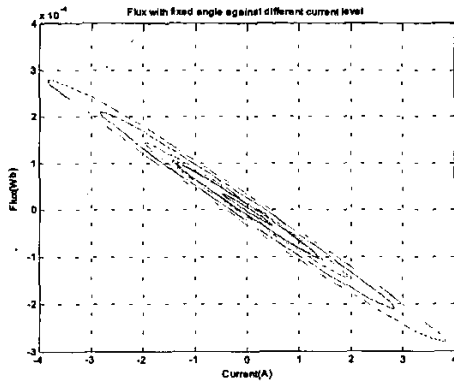


Fig. 15. Hysteresis loops at different current levels

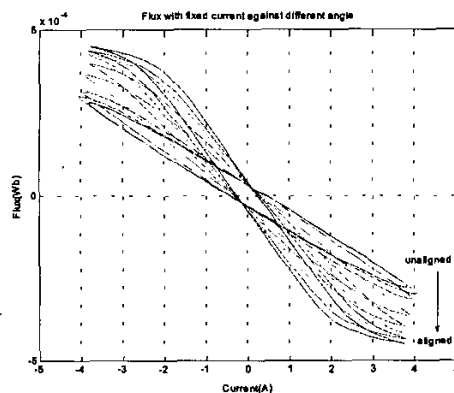


Fig. 16. Hysteresis loops at different angular positions

In Fig. 17, it can be clearly shown that simulation flux is consistent with measured flux values.

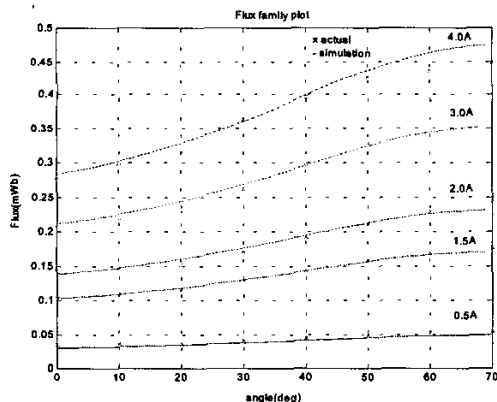


Fig. 17. Comparison between simulation and experimental flux levels

IX. CONCLUSION

This paper describes the detail analysis on the electro-magnetic characteristics of a two-finger VR reluctance gripper. Due to the gripper's compact structure, it was found that the mutual inductances between the fingers cannot be

neglected for the sake of simplicity. Under this circumstance, the magnetic circuit of the gripper is constructed by considering the principal reluctance variation, air-gap permeance, fringing effect, and leakage permeance. To include the mutual coupling between the two fingers, the flux paths of individual finger coils are superimposed onto each other to obtain the overall effect. Finally a comprehensive model of the two-finger VR gripper based on all of the above considerations is constructed. To verify the validity of the electro-magnetic model, a hardware prototype of the two-finger VR gripper is constructed. The electro-magnetic characteristics of the gripper are measured by the detection of flux variations through search coils deployed in strategic locations. When the simulation data and the actual measurements are compared with each other, it was found that the two sets of data are very similar. The results verified that the proposed model of the two-finger VR gripper is an accurate representation of the actual device. The proposed model is very useful for the analysis of small VR electro-mechanical devices. It forms a basic tool for the simulation study and control strategy design of the two-finger gripper.

V. REFERENCES

- [1] J.M. Kokernak and D.A. Torrey, "Magnetic Circuit Model for the Mutually Coupled Switched-Reluctance Machine", IEEE Trans. on Mag, March, Vol. 36, No. 2, p500-507, 2000.
- [2] D.Panda and V. Ramanarayanan, "Effect of Mutual Inductance on Steady-State Performance and Position Estimation of Switched Reluctance Motor Drive", IEEE-Indus. Appl. Soc. 34th Annual Meeting, Vol. 4, p2227-2234, 1999.
- [3] S.H.-Y. Li, F. Liang, Y. Zhao and T.A. Lipo, "A Doubly Salient Doubly Excited Variable Reluctance Motor", IEEE Trans. on Indus. Appl., Jan./Feb., Vol.31, No.1, p99-106, 1995.
- [4] A.M. Michaelides and C. Pollock, "Modelling and Design of Switched Reluctance Motors With Two Phases Simultaneously Excited", IEE Proc.-Electr. Power Appl., Sept., Vol. 143, No. 5, p361-370, 1996.
- [5] L. Xu and E. Ruckstadter, "Direct Modeling of Switched Reluctance Machine by Coupled Field - Circuit Method", IEEE Trans. on Energy Conversion, Sept., Vol. 3, No. 3, p446-454, 1995.
- [6] B.C. Mecrow, C.Weiner and A.C. Clothier, "The Modeling of Switched Reluctance Machines with Magnetically Coupled Windings", IEEE Trans. on Indus. Appl., Nov/Dec., Vol. 37, No. 6, p1675-1683, 2001.
- [7] J.W. Ahn, S.G. Oh, J.W. Moon and Y.M. Hwang, "A Three Phase Switched Reluctance Motor with Two-Phase Excitation", IEEE Trans. on Indus. Appl., Sept/Oct., Vol. 35, No. 5, p1067-1075, 1999.
- [8] Fitzgerald, A.E. & Kingsley, Jr., "Electric Machinery," McGraw-Hill, 2nd Edition, 1961.